Modeling Electrolytic Conversion of Metabolic CO_2 and Optimizing a Macrofluidic Electrochemical Reactor for Advanced Closed Loop Life Support Systems

Jesus A. Dominguez[1], Brittany Brown[2], Lorlyn Reidy[3], Peter Curreri[4], Ellen M. Rabenberg [5]
NASA Marshall Space Flight Center, Huntsville, Alabama, 35811

Brian Dennis[6] and Wilaiwan Chanmanee[7]
University of Texas at Arlington, Arlington, Texas, 76019

Kenneth A Burke[8],
NASA Glenn Research Center, Cleveland, Ohio 44135

The International Space Station (ISS) is currently equipped with a complex, heavy, and power consuming system that recovers approximately 50% of O_2 from metabolic CO_2. Future long duration missions will require a sustainable and highly efficient system capable of yielding a minimum of 75% O_2 recovery. A Macrofluidic Electrochemical Reactor (MFECR) technology development effort is currently underway at NASA Marshall Space Flight Center (MSFC) to significantly increase current O_2 recovery efficiency and reduce complexity of the system. This paper presents a comprehensive multi-physic 3D model developed at MSFC on CO_2 conversion to O_2 and C_2H_4 at standard conditions via MFECR. The 3D spatial domain of the model is a replica of the actual MFECR's 3D drawing generated for the MFECR fabrication and operated to recover O_2 from CO_2 yielding C_2H_4 as byproduct. Electrochemical (EC) physics that includes EC multicomponent reaction mechanisms, mass transport, and current density distributions is coupled in the model with all the other physics phenomena involved in the process, such as free and porous fluid flow, multicomponent mass transfer, heat transfer, and DC electrical current generation along with Joule heating effect. The authors plan to use experimental results to validate this comprehensive and rigorous model and build a reliable simulator that will not only assist the authors on the MFECR design but also optimize its operation.

Nomenclature

AR	=	atmospheric revitalization
CDRS	=	carbon dioxide reduction system
CL	=	catalysis layer
EC	=	electrochemical
CO_2	=	carbon dioxide
C_2H_4	=	ethylene
EDU	=	engineering design unit

[1] Electrolysis Engineer, ECLSS Development Branch, Mail Stop: ES62, MSFC, AL 35812.
[2] ECLSS Engineer/PI, ECLSS Development Branch, Mail Stop: ES62, MSFC, AL 35812.
[3] Ionic Liquids Chemist, Materials Science & Metallurgy Branch, Mail Stop: EM22, MSFC, AL 35812.
[4] Materials Engineer, Materials Science & Metallurgy Branch, Mail Stop: EM22, MSFC, AL 35812.
[5] Materials Engineer, Materials, Test, Chemical & Contamination Control Branch, Mail Stop: EM22, MSFC, AL 35812.
[6] Associate Professor, Dept. of Mechanical & Aerospace Engineering, 701 S. Nedderman Dr. Arlington, TX 76019.
[7] Research Associate, Dept. of Mechanical & Aerospace Engineering, 701 S. Nedderman Dr. Arlington, TX 76019..
[8] Electrical Engineer, Photovoltaic & Electrochemical Systems Branch, Mail Stop: LEX0, 21000 Brookpark RdCleveland, OH 44135.

ECLS = environmental control and life support system
GC = gas chromatograph
GDL = gas diffusion layer
GDE = gas diffusion electrode
MFECR = macrofluidic electrochemical reactor
MPL = macropore layer
MSFC = Marshall Space Flight Center
NASA = National Aeronautics and Space Administration
OGA = oxygen generation assembly
O_2 = oxygen
PDE = partial differential equations
Pt = Platinum
PTFE = poly-tetra-fluoro-ethylene
H_2 = hydrogen
IDE = integrated development environment
IO = inlet-outlet
ISS = international space station
UTA = university of Texas at Arlington
TCC = trace contaminant control

I. Introduction

Atmospheric Revitalization (AR) is the term NASA uses to embrace the engineered systems that maintain a safe, breathable gaseous atmosphere inside a habitable space habitat. An AR system is a key part of the Environmental Control and Life Support (ECLS) system for habitable space habitats. The critical objective for the AR system is to 'close the loop', that is, to capture gaseous human metabolic products, specifically water vapor and CO_2, for maximum O_2 recovery and to make other useful resources from these products. The AR subsystem also removes trace chemical contaminants from the habitat atmosphere to preserve habitat atmospheric quality, provides O_2 and may include instrumentation to monitor cabin atmospheric quality. Long duration crewed space exploration missions will require critical advancements in AR process technologies in order to increase efficiency on O_2 recovery and reduce power consumption as well as mass to increase reliability compared to those used for shorter duration missions that are typically limited to Low Earth Orbit. The AR in the International Space Station (ISS) includes four integrated units, which provide critical functions for life support including trace contaminant control (Trace Contaminant Control (TCC) system), CO_2 removal (CO_2 Removal Assembly (CDRA)), oxygen generation (Oxygen Generation Assembly (OGA)), and oxygen recovery (Carbon Dioxide Reduction System (CDRS)).

CDRS is a Sabatier reactor that operates 300–400 °C and reduces CO_2 to CH_4 and water using H_2 from OGA (an electrolysis unit that generates O_2 as main product and H_2 as byproduct) as reactant. The CDRS limits the feasibility of having a closed loop system, as it requires more water than the water metabolically generated ultimately resulting in a recovery rate of approximately 50%. NASA Marshall Space Flight Center (MSFC) and the University of Texas at Arlington (UTA) are currently developing an Engineering Development Unit (EDU) of a Microfluidic Electro Chemical Reactor (MFECR) to convert a continuous stream of CO_2 and water into O_2 and C_2H_4 at standard conditions. The novel design combines CO_2 conversion and water electrolysis (currently conducted in OGA and CDRS units respectively) into one compact unit that runs at standard conditions and is theoretically capable of generating O_2 with a maximum metabolic CO_2 conversion of 73% while consuming less than metabolic water. The metabolic CO_2 conversion process that currently operates at the ISS yields CH_4 as byproduct losing 4 moles of H (2 moles of H_2 originally generated by 2 moles of water) per 1 mole of C; the novel design yields C_2H_4 as byproduct losing half of the H/H_2 moles than the current CH_4-byproduct-producer approach.

NASA MSFC researchers have developed a rigorous and comprehensive 3D multi-physics model to simulate the EC selective conversion of metabolic CO_2 to C_2H_4 and O_2 at ambient conditions in the MFECR built at an Engineering Design Unit (EDU) scale. All 3D drawings generated to fabricate the different components of the MFECR's EDU were used without modifications or simplification to build the respective 3D model's domains and replicate the actual EDU. In the model, the EC physics (CO_2 conversion to C_2H_4 and formation of H_2 on the cathode in parallel with formation of O_2 on the anode) is coupled with all the other physics phenomena involved in the process. These physics phenomena include fluid flow and mass transfer of reactant/product species in free and porous media, convective/conduction/radiative heat transfer, and conduction of DC electrical current with Joule heating generation.

The MFECR's test stand is fully automated and equipped with a number of inline measurement (flow, pressure, temperature, pH, concentration) systems on all six MFECR's IO streams allowing reliable experimental validation of the model and parametric determination of all EC reactions. Three key EC reactions are considered in the model, two in the cathode (CO_2-C_2H_4 reduction and H_2 formation) and one on the anode (O_2 formation). The authors will use the experimentally validated model as a valuable simulation tool to assist them on the evaluation of the MFECR's design and optimization of its operation.

II. Process Fundamentals

The EC process is conducted via an alkaline electrolyte (KOH) yielding two key competing reactions in the cathode, reduction of CO_2 to C_2H_4 and the formation of H_2 coupled with one reaction in the anode, formation of O_2. EC reactions posted below indicates OH^- is generated in the cathode in the reduction of CO_2 to C_2H_4 and consumed in the anode in the formation of O_2.

Cathode:

$$2CO_2 + 8H_2O + 12e^- = C_2H_4 + 12OH^- \quad (1)$$

$$12H_2O + 12e^- = 6H_2 + 12OH^- \quad (2)$$

Anode:

$$24OH^- = 6O_2 + 12H_2O + 24e^- \quad (3)$$

Total:

$$2CO_2 + 8H_2O = C_2H_4 + 6H_2 + 6O_2 \quad (4)$$

Figure 1 depicts a schematic of the EC process in the MFECR equipped with three flow streams that carry cathodic CO_2 reactant, KOH solution electrolyte, and anodic O_2 product respectively along with two conducting Gas Diffusion Electrodes (GDE) that have two layers, the Gas Diffusion Layer (GDL) and the Catalysis Layer (CL). In the cathode channel CO_2 diffuses through the GDL reaching the CL (coated with copper based catalysis and in direct contact with the electrolyte flow stream) and yielding two EC reactions, CO_2 reduction to C_2H_4 (reaction 1) and H_2 formation (reaction 2). CO_2 and H_2 products diffuse back to the cathode channel mixing with unreacted and depleted CO_2 gas stream. In the anode channel O_2 is generated (reaction 3) at the CL (coated with platinum and in direct contact with electrolyte flow stream) and diffuses throughout the GDL reaching the O_2 flow stream. As indicated in reaction 4, CO_2 reduction reaction consumes water to yield C_2H_4, H_2 and O_2 leading to an increment in OH^- concentration and requiring water makeup to keep the desired OH^- concentration in the electrolyte. Researchers have reported other competing reactions on the cathode yielding different C_1 and C_2 products with copper-based catalysis[1]; UTA researchers have developed a unique and proprietary copper-based catalysis that selectively yields C_2H_4 against CO and CH_4[2]. The model neglects CO and CH_4 products in the cathode as their compositions in the outlet stream have shown to be lower than 2%.

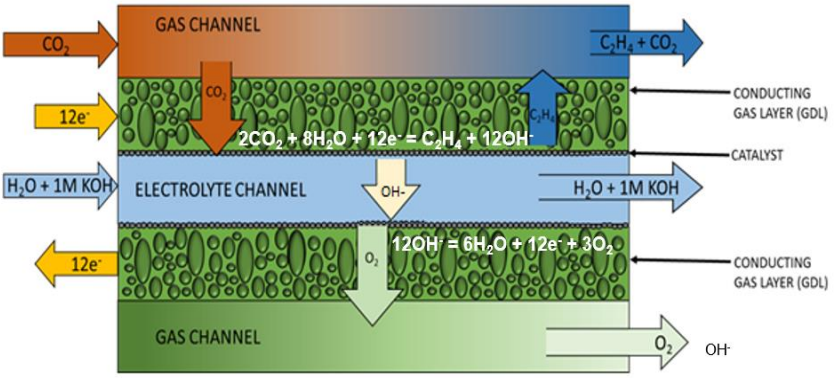

Figure 1. Schematic of EC process in the MFECR.

III. Model Domains

The 3D drawings generated to fabricate the five key MFECR's components are used as the model's spatial domains to replicate the actual MFECR's three-dimensional geometry at EDU scale. The five MFECR components include two non-electrical-conducting endplates, two electrical-conducting serpentine channels, and one non-electrical-conducting electrolyte serpentine channel. Two additional spatial domains, cathode and anode GDEs, are replicated

based on the dimensions specified by the manufacture. The GDE domain consists of three subdomains, the gas diffusion layer (GDL), the microporous layer (MPL), and the catalytic layer (CL). MPLs are typically built up by a mixture of carbon black powder and a hydrophobic agent, typically poly-tetra-fluoro-ethylene (PTFE).

These seven spatial domains are stacked having one top endplate followed underneath by the cathode section (consisting in one serpentine chamber and the GDE), the electrolyte serpentine chamber, the anode section (consisting in one serpentine chamber and the GDE), and finally the bottom endplate. Besides the seven spatial domains described above, the model also includes three flow domains, CO_2 gas, electrolyte liquid, and O_2 gas flowing through the cathode, electrolyte, and anode serpentine channels respectively.

Figure 2 depicts a) the complete MFECR stack having both, the top and bottom endplates colored in purple, b)

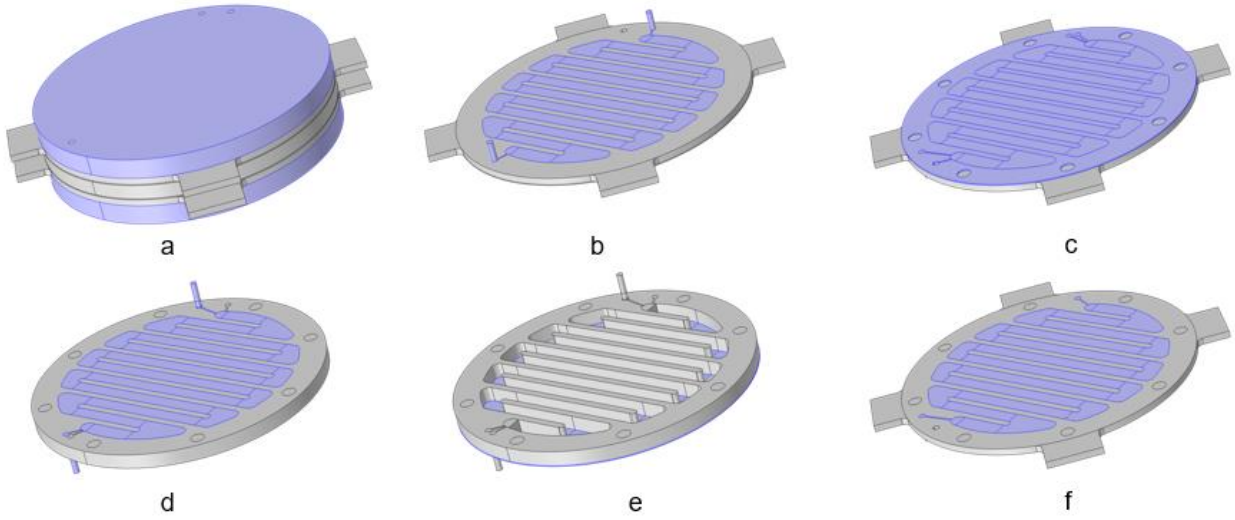

Figure 2. MFECR's model domians: a) top and bottom endplates (both purple), b) cathode channel and CO_2 flow (purple), c) cathode GDE (purple), d) electrolyte channel and alkaline solution flow (purple), e) anode GDE (purple), f) anode channel and O_2 flow.

CO_2 gas flowing (purple) through the cathode serpentine channel, c) cathode GDE (purple), d) electrolyte solution flowing (purple) through the electrolyte serpentine channel, e) anode GDE (purple), and f) O_2 gas flowing (purple) through the anode serpentine channel. The materials used in the actual MFECR elements and assigned to the corresponding model's material domains include polycarbonate for the endplates, Teflon for the electrolyte serpentine channel, nickel for the anode and cathode serpentine channels, and porous carbon-based composite for the GDE.

Figure 3 illustrates the flow domains and the direction of the IO flow streams in each serpentine channel

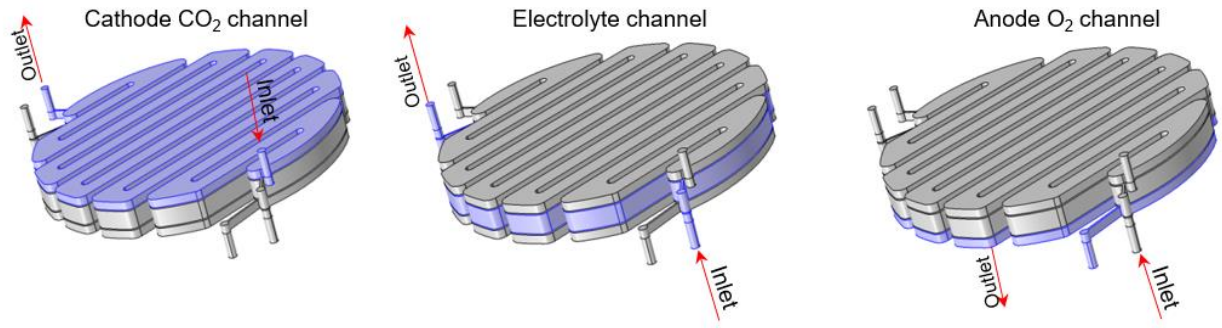

Figure 3. Flow domains and I/O streams for the cathode, electrolyte, and anode serpentine channels.

corresponding to the cathode (CO_2 gas), electrolyte (liquid KOH solution), and anode (O_2 gas).

IV. Model Definition

The EC reaction section of the MFECR is constructed with two porous gas diffusion electrodes (GDEs) with an electrolyte sandwiched in the middle as shown in Figure 3. The CO_2 feeds in the cathode serpentine chamber and part of the O_2 product is fed back to the anode serpentine chamber. The alkaline solution feeds the electrolyte serpentine chamber wetting the CLs of both the anode and cathode GDEs and allowing ionic transport between them. The EC reactions in the cell are reactions (1) and (2) in the cathode's GDE and reaction (3) in the anode's GDE.
The model includes the following processes:

- Electronic charge balance (Ohm's law)
- Ionic charge balance (Ohm's law)
- Butler-Volmer charge transfer kinetics
- Flow distribution in gas and liquid channels (Navier-Stokes)
- Flow in the porous GDEs (Brinkman equations)
- Mass balances in gas phase in both gas channels and porous electrodes (Maxwell-Stefan diffusion and convection)
- Temperature (energy balance equation) via three types of heat transfer mechanisms, conductive within MFECR's components, convective within the channel flows and MFECR-ambient interface, and radiative to/from the ambient.
- Heat generation/source via Joule heating effect.

A. Charge Balances

The electronic and ionic charge balance in the cathode and anode current feeders, the electrolyte and GDEs are solved for using a secondary current distribution interface that accounts for the effect of the electrode kinetics in addition to solution resistance. The model assumes that concentration-dependent Butler-Volmer charge transfer kinetics describes the charge transfer current density. At the cathode, CO_2 is reduced to C_2H_4 and H_2 as stated in reactions (1) and (2) respectively, assuming the first electron transfer to be the rate-determining step, the following charge transfer kinetics equations apply for reactions (1) and (2) respectively:

$$i_{c,co_2} = i_{o,co_2}\left(\frac{c_{co_2}}{c_{co_2,ref}} exp\left(\frac{\alpha_{c,co_2}F}{RT}\eta\right) - \frac{c_{c_2h_4}}{c_{c_2h_4,ref}} exp\left(\frac{-\alpha_{a,co_2}F}{RT}\eta\right)\right) \quad (5)$$

$$i_{c,h_2} = i_{o,h_2}\left(\frac{c_{h_2}}{c_{h_2,ref}} exp\left(\frac{\alpha_{c,h_2}F}{RT}\eta\right) - exp\left(\frac{-\alpha_{a,h_2}F}{RT}\eta\right)\right) \quad (6)$$

Here i_{o,co_2} and i_{o,h_2} are the cathode exchange current densities (A/m^2) for the cathode reactions (1) and (2), c_{co_2} $c_{c_2h_4}$ c_{h_2} are the molar concentrations of CO_2, C_2H_4, and H_2 respectively, $c_{co_2,ref}$ and $c_{c_2h_4,ref}$ are the reference concentrations (mol/m^3). α_{c,co_2} α_{a,co_2} α_{c,h_2} α_{a,h_2} are the cathodic/anodic charge transfer coefficients for the cathode reactions (1) and (2). Furthermore, F is Faraday's constant (C/mol), R the gas constant (J/(mol·K)), T the temperature (K), and η the overpotential (V).

For the anode, the following charge transfer kinetics equation applies for reaction (3)

$$i_{c,o_2} = i_{o,o_2}\left(\frac{c_{o_2}}{c_{o_2,ref}} exp\left(\frac{\alpha_{c,o_2}F}{RT}\eta\right) - exp\left(\frac{-\alpha_{a,o_2}F}{RT}\eta\right)\right) \quad (7)$$

Here i_{o,o_2} is the anode exchange current density (A/m^2) for the anode reaction (3), c_{o_2} is the molar concentration of O_2, $c_{o_2,ref}$ is the reference concentration (mol/m^3). α_{c,o_2} α_{a,o_2} is the cathodic/anodic charge transfer coefficients.
The overpotential η is defined as

$$\eta = \Delta\phi_{electronic} - \left(\Delta\phi_{ionic} + \Delta\phi_{eq}\right) \quad (8)$$

Where $\Delta\phi_{eq}$ is the equilibrium potential difference (SI unit: V). The concentration-dependent kinetics expressions (5), (6) and (7) are used to set up the charge transfer expressions that lead to $\Delta\phi_{ionic}$ value.

At the cathode's inlet boundary, the potential is set at a reference potential of zero (ground). At the anode's inlet boundary, the potential is set to the cell potential V_{cell}. The cell polarization V_{pol} is then given by

$$V_{pol} = \left(\Delta\phi_{eq,c} - \Delta\phi_{eq,a}\right) - V_{cell} \quad (9)$$

Where $\Delta\phi_{eq,c}$ and $\Delta\phi_{eq,a}$ are the total equilibrium differential potential of all individual species participating in the EC reactions on the cathode and the anode respectively.

B. Multicomponent Transport

At the cathode serpentine channel, CO_2 gas is supplied as reactant, meaning that the gas in the channel and GDE consists of three components: unreacted CO_2 and products C_2H_4, and H_2. In the anode, O_2 product is resupplied, consisting of two product components: O_2 and water vapor.

The material transport is described by the Maxwell-Stefan's diffusion and convection equations, solved for by using a transport of concentrated species interface for each electrode flow serpentine channel. The boundary conditions at the walls of the gas channel and GDE are zero mass flux (insulating condition). At the inlet, the composition is specified, while the outlet condition is convective flux. This assumption means that the convective term dominates the transport perpendicular to this boundary. Continuity in composition and flux apply for all mass balances at the interfaces between the GDEs and the serpentine channels.

C. Gas and Liquid Flow Equations

The Brinkman Equations interface is used for solving the velocity field and pressure in both the cathode and anode serpentines channels. The compressible Navier-Stokes equations govern the flow in the open channel sections and the Brinkman equations in the porous GDEs. Couplings for the density, velocity, pressure and net mass sources and sinks are made to the transport of concentrated species interfaces by using reacting flow multiphysics. The incompressible Navier-Stokes equations govern the liquid flow in the electrolyte serpentine channel.

D. Heat Transfer Equations

A general energy balance equation is implemented in the model to obtain the temperature distribution throughout the MFECR including all solid parts and three flows running through the cathode, anode, and electrolyte serpentine channels. The model takes into account two heat transfer mechanisms for the heat exchange between the MFECR's surface and the ambient, natural convection and thermal radiation. In the natural convection, a constant heat transfer coefficient is originally assumed based on values found in the literature, the plan is to actually find it via experimental validation by measuring temperature throughout the MFECR's surface. Radiation emissivity of the MFECR's materials are found in the literature and used in the model to compute the radiative heat transfer mechanism between MFECR's surface and the ambient.

As a potential is applied between the two GDE's, an electrical current is generated and carried throughout the walls of the cathode, anode, and electrolyte serpentine channels, the model accounts for this source of energy transformed in heat generation via the Joule heating effect equation.

V. Results and Discussion

The model and simulation was implemented in COMSOL[3], a cross-platform finite element analysis, solver and multiphysics simulation software. It allows conventional physics-based user interfaces and coupled systems of partial differential equations (PDEs). COMSOL provides an integrated development environment (IDE) and unified workflow for electrical, mechanical, fluid, acoustics and chemical applications. The complexity and the number of coupled multiphysics involved in the model lead to demanding significant computational power; a typical run case of the model requires 45-60 MB of RAM.

Figure 4 depicts the modeled potential profile throughout the GDEs and the electrolyte as a differential potential of 2.5 V is applied between the cathode and anode GDE's. The potential actually is applied to the ears of the cathode and anode serpentine channels (shown in Figure 2a) spreading through the GDEs as they

Figure 4. MFECR's model results: Potential (V) profile throughout GDEs and electrolyte

are electrically conductive. Due to the fact that the nickel-made serpentine channels have dissimilar electrical conductivity than the carbon-based GDEs, a differential potential is generated between both materials leading to a lower potential applied to the cell; the model accounts for this potential differential as it includes both domains having the potential applied as boundary conditions on the serpentine channels.

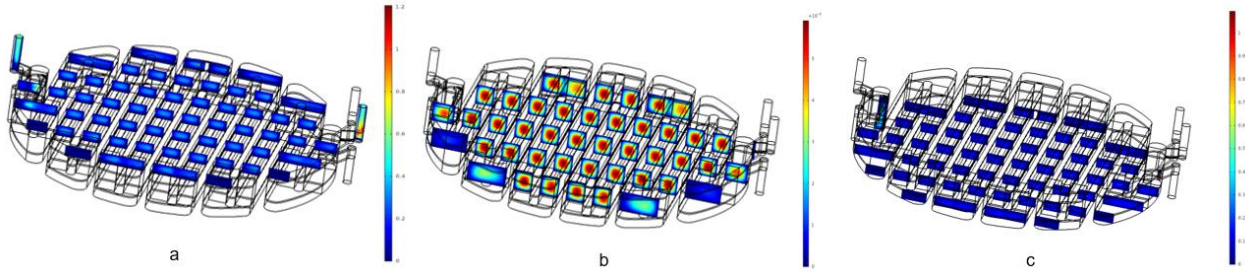

Figure 5. MFECR's model results: Flow velocity (m/s) profile throughout the a) cathode, b) electrolyte, and c) anode serpentine channels.

Figure 5 depicts the modeled flow velocity profile throughout a) the cathode, b) electrolyte, and c) anode serpentine channels. The Brinkman equation is used for solving the velocity field and pressure in both the cathode and anode serpentines channels as these flows have two regimes, free flow in the hollow channel and porous flow in the GDE.

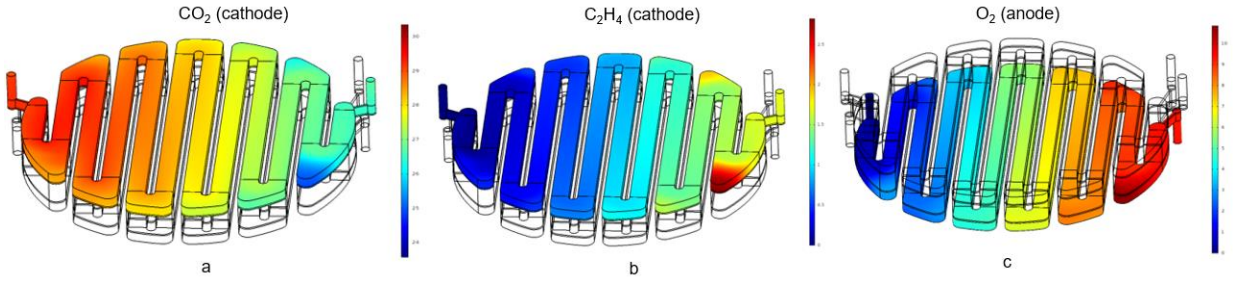

Figure 6. MFECR's model results: a) CO_2 and b) C_2H_4 compositions (mol/m^3) profile throughout the cathode serpentine channel and c) O_2 composition profile throughout the anode serpentine channel

Figure 6 depicts the concentration profile of a) CO_2 and b) C_2H_4 throughout the cathode serpentine channel, CO_2 depletes at expenses of the C_2H_4 generation enriching the cathode gas flow with C_2H_4 as the CO_2 continues reacting and flowing toward the channel's end.

A secondary product generated along the cathode serpentine channel is H_2 (omitted in Figure 6) that as C_2H_4, once is generated on the CL coated with copper-based catalysis, it diffuses through the GDL to reach the serpentine channel and mix with the flowing CO2 gas. On the anode serpentine-channel side, O_2 is generated on the CL coated with Platinum (Pt) and diffused through the GDL reaching the carrier gas used to feed the anode serpentine channel.

Figure 7 depicts the temperature profile of the a) MFECR's surface and b) KOH electrolyte solution flow that is fed at 277 K having set at an ambient temperature of 300 K. The model takes into account two sources of heat exchange with the environment (natural convection and thermal

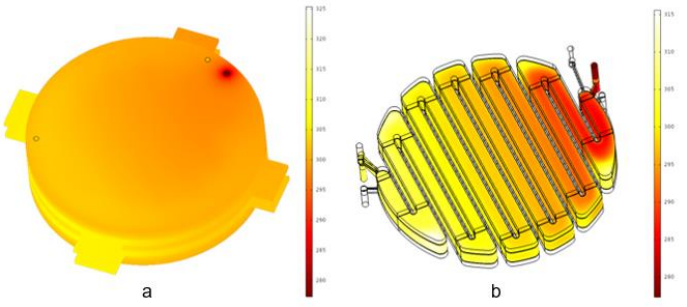

Figure 7. MFECR's model results: Temperature (K) profile throughout the a) MFECR's surface and b) electrolyte serpentine channel as KOH solution is fed to the electrolyte serpentine channel at 277 K having an ambient temperature of 300 K.

radiation) as well as one heat source (Joule heating effect). The model uses different constant natural convective heat transfer coefficient on three MFECR's surface area, two (horizontal and vertical) open areas and one horizontal underneath area. The value of each of these three coefficients will be experimentally determined through validation by measuring temperature throughout the MFECR's surface.

As illustrated in Figure 7a, the cold electrolyte feed stream generates a cold spot on the MFECR's endplate surface. Figure 7b shows that the electrolyte temperature increases as the KOH solution flows toward the electrolyte channel's exit due mainly to heat flux gain from not only the ambient but also the Joule-heating effect.

Joule heating is the physical effect by which the pass of current through an electrical conductor produces thermal energy. This thermal energy is then evidenced through a rise in the conductor material temperature, thus the term "heating". Joule heating is a transformation between "electrical energy" and "thermal energy", following the energy conservation principle.

Figure 8 depicts the volumetric power (W/m^3) generated throughout both the MFECR's cathode and anode serpentine channels due to the Joule heating effect. As illustrated in Figure 8, abrupt high volumetric power (red regions) happen to be on the sharp angles formed on the joint sections of not only the ears with the serpentine-channel body but also the serpentine-channel wall and the GDL's upper surface. . .

As electrical potential is actually applied on each of the four ears of both (cathode and anode) serpentine channels and not on the GDE's.); actual potential value happens to be lower because the two joint materials (nickel-based channel and carbon-based GDE) have different density and electrical conductivity. The model correctly sets the experimental operating potential value as boundary conditions on the ear's surface (dark red and dark blue regions. In Figure 9 a potential of 2.5 V is applied to each of the four ears of the cathode serpentine channel (dark red region) while ground (0 V) is applied to the anode (dark blue). The modeled electrical potential decreases substantially on the GDE that is the floor of the serpentine channel, from 2.5 V to 1.6 V (light yellow region) near the body-channel wall and 1.4 V (light green) along the serpentine channel estimates the electrical potential.

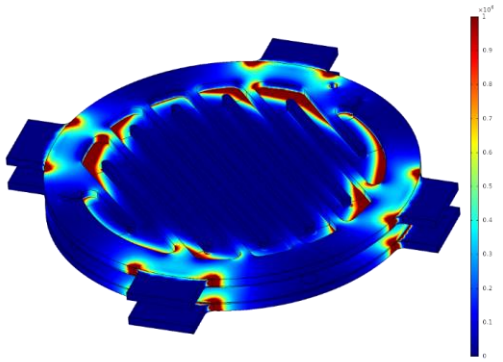

Figure 8. MFECR's model results: Heat generation (W/m^3) via Joule heating on serpentine channels and GDEs as a potential difference of 2.5 V is applied to channel's ears.

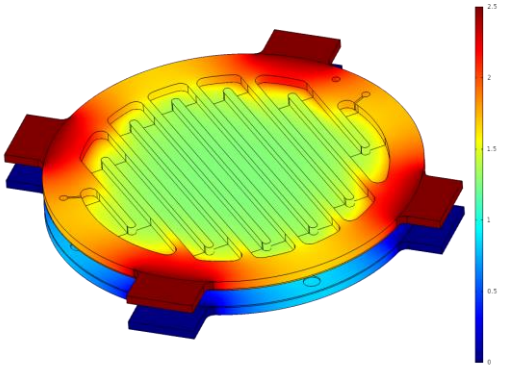

Figure 9. MFECR's model results: Electrical potential on serpentine channels and GDEs as a potential difference of 2.5 V is applied to the channel's ears.

VI. Model Validation

The model presented in this paper has the foundations and rigor to simulate the actual EC process allowing the user to optimize the design and operation of the MFECR and efficiently deliver metabolic CO_2 reduction to C_2H_4 generating H_2 and O_2 as byproduct at ambient conditions. The MFECR is installed in a test stand at MSFC equipped with all the instrumentation and sensors that will allow fully validation of the model including determination of the EC kinetics parameters for the key EC reactions that take place on the cathode and the anode.

All inlet-outlet (IO) streams of the MFECR are fully monitored inline yielding flow rate, temperature, and pressure for all IO streams along with pH on both input and output KOH solution streams as well as gas composition on the cathode and anode outlet streams. The IO streams include the inlet CO_2 gas and outlet product streams at the cathode channel, the inlet O_2 carrier gas and the outlet product streams at the anode chamber, and the inlet and outlet KOH-solution streams.

A set of thermocouples distributed throughout the entire MFECR's surface will be used to experimentally validate the heat transfer part of the model and determine key parameters, such as the heat transfer coefficient via natural convective heat transfer between the MFECR's surface and the ambient.

Acknowledgments

Special thanks to Dr. Enrique Jackson for his support and assistance on the use of a high-performance computational system (512 Mb of RAM) that has allowed us to run the model in hours rather than days. We are also thankful to Allison Burns and Samantha Hall for their contribution on the model development during their internship at MSFC.

References

[1] Y. Hori: Electrochemical CO_2 reduction on metal electrodes. In Modern Aspects of Electrochemistry, Vol. 42, C.G. Vayenas, R.E. White, and M.E. Gamboa-Aldeco, eds. (Springer, New York, 2008); pp. 89-189.

[2] Tacconia N. R., Chanmanee W., Dennis B., Rajeshwarb K., Composite copper oxide–copper bromide films for the selective electroreduction of carbon dioxide, J. Mater. Res., Vol. 32, No. 9, May 15, 2017; pp. 1727-1724

[3] COMSOL, Electrochemistry Module User's Guide, Software Manual – User Guide, Version: COMSOL 5.4, 2018. https://doc.comsol.com/5.4/doc/com.comsol.help.echem/ElectrochemistryModuleUsersGuide.pdf